23 April 1982, Volume 216, Number 4544 **SCIENCE**

Surface Spectroscopies with Synchrotron Radiation

N. V. Smith and D. P. Woodruff

Synchrotron radiation is the light emitted by high-energy electrons as they are accelerated in the bending magnets of high-energy machines such as storage rings. It forms a continuum from the infrared to the x-ray region and is emitted in a highly collimated beam. The availability of this radiation to spectroscopists over the past decade has affected physics, chemistry, biology, and materials science (*1*). New storage rings are under construction which are dedicated to, and specially designed for, the production of synchrotron radiation. Three new rings are being built in the United States: two rings with energies of 2.5 and 0.7 billion electron volts (GeV) at the National Synchrotron Light Source (NSLS) at Brookhaven National Laboratory, and the 1.0-GeV ALADDIN ring at the University of Wisconsin–Madison. It is expected that the new sources will extend substantially the capabilities of all the optical and x-ray spectroscopies in which synchrotron radiation is now used. In this article we address one of the many areas under study, namely the investigation of solid surfaces, presenting a few highlights of recent research and trying to extract the promising future trends. We also speculate on some of the qualitatively new experiments that should become possible.

Summary. A variety of photoelectron spectroscopies using synchrotron radiation have been devised to study solid surfaces. Measurements of the energies and angular distributions of electrons photoemitted from valence levels yield detailed information on surface electronic states and the chemical bonding of adsorbed atoms and molecules. Core level studies yield surface atom positions and molecular orientations. Some highlights of recent research are presented here. The capabilities of the techniques will be extended by the forthcoming generation of new storage rings dedicated to the production of synchrotron radiation.

The specific surface characterization technique on which we concentrate is photoemission spectroscopy and its various derivatives. The basic physics of the photoemission process is illustrated in Fig. 1. A sample is irradiated with photons of energy $\hbar\omega$, generating photoelectrons, which are emitted into a vacuum (photoelectric effect). The energy spectrum is, to some approximation, a replica of the occupied density of electronic states; thus photoemission is a powerful means of elucidating electronic energy levels. Some of the features of the spectrum in Fig. 1 have been given labels according to the subsidiary photoemission technique that derives from their study. Photoemission is therefore not a single spectroscopy, but a range of spectroscopies sharing similar instrumentation. We list in the following sections a number of these spectroscopies and the nature of the information they provide.

The surface sensitivity of the photoemission technique arises because of the short lifetime of the photoelectron due to inelastic scattering with unexcited electrons. Depending on the electron energy, typical lifetimes correspond to mean free paths in the range 5 to 20 angstroms, not much larger than interatomic spacings. There are two major consequences, both of which are indicated in Fig. 1. First, photoelectrons originating from deep within the solid are lost, and this means that the signal from the surface atomic layers can be comparable with that from the bulk. Second, photoelectrons that have undergone one or more inelastic scatterings may still escape from the surface, and this gives rise to an inelastic background and the extreme low-energy peak in the spectrum.

Photoemission Spectroscopies

Valence UPS. The most energetic photoelectrons are those emitted elastically from the valence states of the solid surface. Traditionally, these were studied with laboratory ultraviolet light sources ($\hbar\omega \lesssim 40$ electron volts) leading to the technique named ultraviolet photoelectron spectroscopy (UPS). For solids, the spectra can be compared with densities of states calculated from the theoretical bulk band structure. For adsorbates, the energy locations of peaks can be compared with calculated binding energies for surface complexes and clusters. The spectrum also serves as a fingerprint for the various molecular species. Clean solid surfaces have surface states distinct from those in the bulk, and their energies can also be measured and compared with theory.

ARUPS. An important refinement of UPS is angle-resolved ultraviolet photoelectron spectroscopy (ARUPS). By measuring the spectra systematically as a function of direction of emission, one obtains the momenta of the photoelec-

---

N. V. Smith is a member of the technical staff at Bell Laboratories, Murray Hill, New Jersey 07974, and is a user of the synchrotron radiation facilities at the University of Wisconsin–Madison and the Brookhaven National Synchrotron Light Source. D. P. Woodruff is lecturer in the Department of Physics, University of Warwick, Coventry CV4 7AL, United Kingdom, and is a user at the Daresbury Synchrotron Radiation Source.

0036-8075/82/0423-0367$01.00/0

trons. This permits detailed mapping of the energy versus wave vector, $E(\mathbf{k})$, dispersion relations—that is, the band structure of solids. The dispersion with parallel wave vector can be observed for clean-surface and adsorbate-induced states. Varying the angle of emission with respect to the polarization vector of the incident radiation permits detailed examination of optical selection rules and orbital symmetry.

ESCA/XPS. Atomic core levels may be observed as sharp peaks in the photoelectron energy spectrum. The measured binding energies are characteristic of the atomic species, and differences in chemical environment for like atoms can be detected as shifts in these binding energies. One of the original names for the technique, electron spectroscopy for chemical analysis (ESCA), coined by Kai Siegbahn, is particularly apt. Core electrons are deeply bound, so that it is necessary to use relatively high photon energies to excite them. Traditionally, this technique was practiced in the x-ray range ($\hbar\omega \gtrsim 1$ kiloelectron volt), leading to the alternative name of x-ray photoemission spectroscopy (XPS). The advent of synchrotron radiation, with its continuum nature, has removed any clear distinction between UPS and XPS. It is useful, nevertheless, to retain the distinction between valence level studies and core level studies. Study of chemical shifts of atoms at surfaces is growing in popularity, and the newly emergent technique might be appropriately called surface ESCA.

PhD. Photoelectron diffraction (PhD) is an angle-resolved photoemission spectroscopy which detects the diffraction experienced by the wave functions of photoelectrons emitted from core levels of adsorbed atoms. This can be done either by monitoring the anisotropy of the emission or by scanning the photon energy, which is equivalent to scanning the photoelectron de Broglie wavelength. The information sought is interatomic distances and site geometry for atoms and molecules adsorbed on surfaces.

SEXAFS. Interatomic distances for adsorbates can also be investigated through the alternative technique of surface-extended x-ray absorption fine structure (SEXAFS). The photon energy is tuned through the characteristic energy for the onset of core level excitation for surface atoms. The core holes thus created can then be filled by nonradiative decay of a higher lying electron and communication of energy to yet another electron, which can then escape from the surface (Auger emission). The photoabsorption can therefore be monitored by direct detection of these Auger electrons or by their substantial contribution (through inelastic loss processes) to the total photoelectron yield. Measurements of the photon energy dependence of either of these will therefore show a step at the threshold energy, and above this step will be the well-known EXAFS oscillations (*2*), whose periodicity gives nearest neighbor distances.

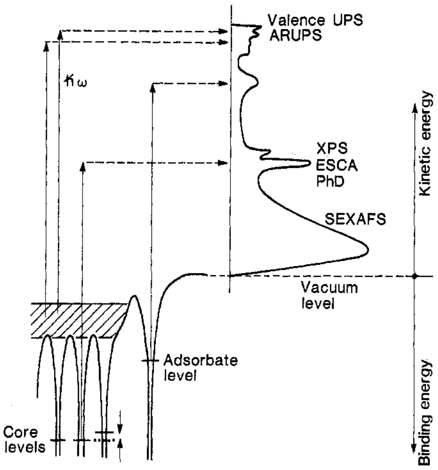

Fig. 1. Basic physics of photoemission from a solid surface, showing the electron potential in the surface region and the energy spectrum of photoemitted electrons at photon energy $\hbar\omega$. The spectrum is labeled with the abbreviations and acronyms of the various subsidiary photoemission spectroscopies.

PSD. If the detected particles are ions rather than electrons, we have the technique of photostimulated desorption (PSD). The photostimulated ion angular distribution (PSDIAD) can yield data on surface atomic bonding geometries which are qualitatively easy to interpret. Some mechanisms of PSD require electronic transitions involving substrate atom core levels, and this gives rise to an interesting variant of SEXAFS.

The special properties of synchrotron radiation are essential to the spectroscopies mentioned above in several ways. Synchrotron radiation has a continuous spectrum, it is intense, and it is highly polarized. A property that has not been extensively exploited so far is the pulsed time structure. What advantages, then, will the new sources offer? The answer, briefly, is intensity and brightness. The new storage rings in the United States have been designed for high brightness. This means that the emitting source of electrons within the bending magnets is very small. The vertical dimensions ($1\sigma_y$ distances) are predicted to be about 100 micrometers—considerably smaller than in present machines. The high brightness facilitates the design of high-efficiency and high-resolution monochromators. There exist practical limits to the problem of matching a source of a certain size and angular spread to a monochromator characterized by a certain entrance slit width and angular acceptance. High brightness is advantageous in terms of the number of photons that can actually be delivered to a sample. Alternatively, for a given flux, the photons can be delivered to a much smaller spot size on the sample surface. This is of importance if one wishes to perform the spectroscopies listed above with spatial resolution. It is also of relevance to improvements in the angular resolution of ARUPS experiments.

Let us now examine a few of the noteworthy recent achievements in surface science experiments made with these synchrotron radiation–based spectroscopies.

Surface ESCA

As indicated in Fig. 1, one expects the binding energy of a core level for an atom in the outermost surface layer to be different from that for an atom in the bulk. This is because the occupancy of valence levels, and hence the atomic potential, will be slightly different. Only recently, however, have such chemical shifts been observed (*3*). The shifts are rather small (~ 0.5 eV), so that good resolution, good cross section, and good surface sensitivity are required to detect them. In Fig. 2 we show some recent data obtained on the Ta(111) and W(111) surfaces (*4*). Only the peaks corresponding to the $4f_{7/2}$ core levels are shown. (The other spin orbit component, $4f_{5/2}$, is well removed in energy.) A peak (labeled B) associated with bulk atoms is observed, as well as peaks (S_1 and S_2) that are attributed, respectively, to first- and second-layer surface atoms.

Interestingly, the sign of the bulk-surface chemical shift reverses at some point along the row of the periodic table between Ta and W. One of the models suggested to explain the shifts proposes that the core level follows the displacement of the valence d-band center of gravity at the surface. The d-band shift itself is caused by the combined effects of band narrowing due to fewer nearest neighbors and a shift in the direction that would restore charge neutrality. The surface d band, and hence the surface core level, moves upward if the Fermi level is above the midpoint in the bulk d band, and vice versa. A more detailed analysis with realistic *d*-band shapes shows that the reversal occurs not when the *d* band is half full, but actually between Ta and W.

Adsorption of hydrogen modifies the core level spectra, as shown in Fig. 2, b and d. The H atoms bond to the surface Ta or W atoms. A small amount of electronic charge flows to the H atoms from the metal substrate, giving rise to S'_1 and S'_2 levels with higher binding energies than S_1 and S_2.

This surface chemical shift spectroscopy is already being used in the study of reconstructed surfaces, oxidation of semiconductor surfaces, and metal overlayers on surfaces (Schottky barrier formation). The increased intensity and energy range available with the new synchrotron sources will make accessible the core levels for elements over more of the periodic table. Advanced monochromators with better resolution will permit greater precision and the detection of even smaller chemical shifts. Perhaps the most important development, however, will be easier access to the energy range above the carbon *K* edge. (The binding energy of the C 1*s* core level is ~ 290 eV.) There is intense interest in the chemical behavior of organic molecules on surfaces, from both a scientific and a technological point of view, because of their relevance to catalysis, atmospheric pollution, and refinement of fossil fuels. We expect greatly increased activity in this area. At present, this energy range is very difficult to work in. Carbon is a universal contaminant in vacuum systems. It accumulates on the surfaces of mirrors and gratings and, ironically, because of the existence of the carbon *K* edge in the absorption, severely degrades their reflecting powers. The high intensity and high brightness of the new sources offer a brute-force solution to this problem.

High *k*-Space Resolution

Angle-Resolved Photoemission

If one measures the kinetic energy E of a photoelectron and its polar angle of emission θ with respect to the surface normal, one has automatically measured the parallel component of its wave vector

$$k_{\parallel} = (2mE/\hbar^2)^{1/2} \sin\theta \qquad (1)$$

where m is the mass of the electron and $\hbar$ is Planck's constant divided by 2π. The surface energy bands, or $E(\mathbf{k}_{\parallel})$ dispersion relations, can thereby be mapped out for surface states, adsorbate states, and three-dimensional bulk band structures. The W(100) surface is particularly rich in the variety of its surface states, and some recent ARUPS data are shown in Fig. 3 (*5*). By testing for extreme sensitivity to surface contamination, three surface state features can be identified: the Swanson hump, designated *SH*; the "doublet" feature, *D*; and the low-lying state, *LL*. Applying Eq. 1, one obtains the $E(\mathbf{k}_{\parallel})$ results of Fig. 3. The energies plotted are the initial-state energies relative to the Fermi energy (actually $E_i = E - \hbar\omega + \Phi$, where Φ is the work function). The $\bar{\Sigma}$ line in the surface Brillouin zone has mirror symmetry, and by varying the polarization orientation of the incident radiation it has been possible to distinguish states of odd and even parity (crosses and circles, respectively, in Fig. 3). Theoretical band calculations (*6*) for this surface yield recognizably

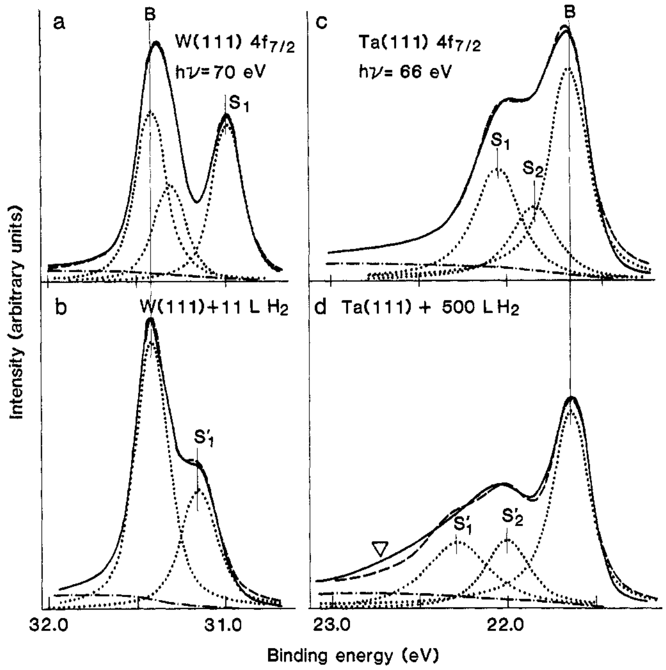

Fig. 2. Photoelectron energy spectra in the region of the $4f_{7/2}$ core level for W(111) and Ta(111), both clean (a and c) and with a monolayer coverage of hydrogen (b and d). The chemically shifted core levels for first- and second-layer atoms (S_1 and S_2) are resolvable from the bulk core level *B*. The surface chemical shifts are modified by bonding with H. The amounts of hydrogen to which the surfaces in (b) and (d) were exposed were 11 and 500 langmuirs (1 L = 10^{-6} torr for 1 second). [From van der Veen *et al.* (*4*)]

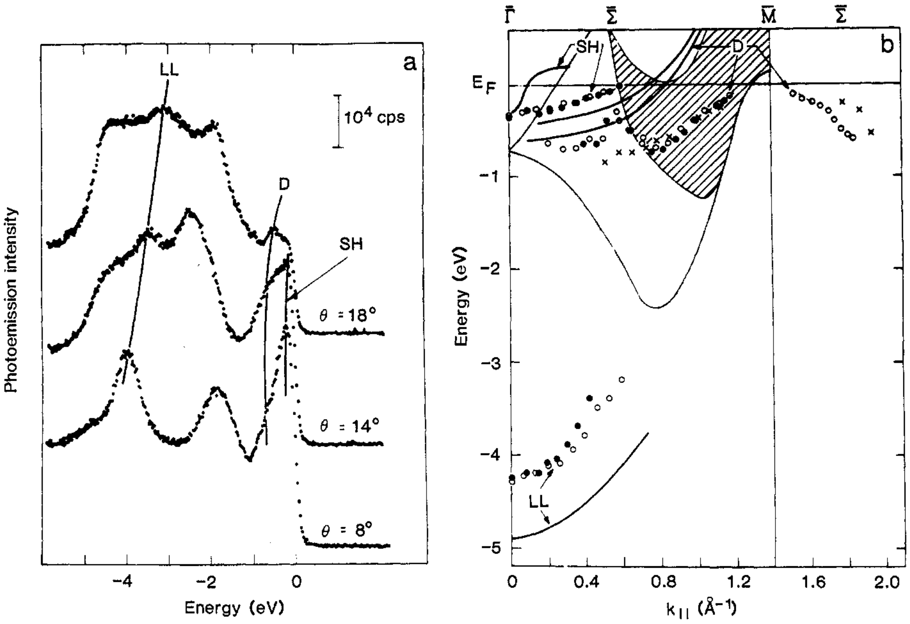

Fig. 3. (a) Photoelectron energy spectra in the valence band region on the W(100) surface show surface state features *LL*, *D*, and *SH*, which move as a function of angle of collection θ. (b) Experimental $E(\mathbf{k}_{\parallel})$ dispersion relations (circles and crosses) derived from the spectra. The full curves labeled *LL*, *D*, and *SH* are the corresponding curves obtained in theoretical calculations. Also shown is the absolute gap (hatched) of the bulk band structure. [From Holmes and Gustafsson (*5*)]

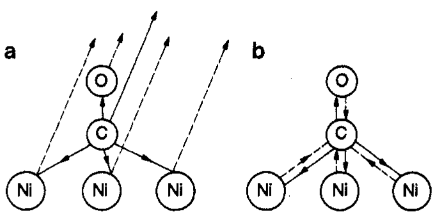

Fig. 4. Interference effects in the wave function of photoelectrons emitted from adsorbate core levels, in this case the carbon 1*s* level for CO adsorbed on a nickel surface. The waves scattered from surrounding atoms (dashed arrows) interfere with the directly emitted wave (full arrows): (a) photoelectron diffraction case; (b) SEXAFS case.

similar surface states, but a comparison of the $E(\mathbf{k}_\parallel)$ relations (shown in Fig. 3) reveals substantial differences in detail.

At low temperature, the W(100) surface is known to undergo a reconstruction to a $c(2 \times 2)$ arrangement, in which the repeat distance for the unit cell of the surface atoms is twice that for the underlying bulk. The fact that the theoretical $E(\mathbf{k}_\parallel)$ curve for the *D* surface states crosses the Fermi level very close to the halfway point in the Brillouin zone has lent support to the idea that the reconstruction is driven by a Peierls instability or charge density wave mechanism (*7*). The data of Fig. 3, however, show that the experimental feature identified with *D* crosses the Fermi level at a point significantly removed from the halfway point, thus obligating us to question this mechanism.

Studies of this kind have been performed on many adsorbate systems. The continuous nature of $\hbar\omega$ has permitted studies of bulk band structures of solids throughout the entire three-dimensional Brillouin zone.

For future studies of this kind it will be desirable to work with improved *k*-space resolution. From Eq. 1 it follows that

$$\Delta k_\parallel = (2mE/\hbar^2)^{1/2} \cos\theta\Delta\theta \qquad (2)$$

For the case just considered, the angular aperture $\Delta\theta$ was 5° and *E* varied over the range 9 to 17 eV. This corresponds to a *k*-space resolution in the range 0.13 to 0.18 Å^{-1}, which is to be compared with the Brillouin zone width $\overline{\Gamma M} = 1.4\ \text{Å}^{-1}$. This is adequate for the purpose at hand. At higher photon energies the resolution deteriorates at $E^{1/2}$. But, more important, there are many surfaces that undergo reconstruction on much larger scales—for instance, Si(111), 7 × 7; Au(100), 5 × 20; and Ge(111), 2 × 8. ARUPS studies must therefore be able to resolve features on a scale appropriate to the much smaller Brillouin zones. The new synchrotron radiation sources are well matched to this purpose. The high brightness permits the delivery of many photons to a very small spot on the sample, so that it should be possible to use extremely small angular apertures (~ 0.5°) and still have tolerable signals.

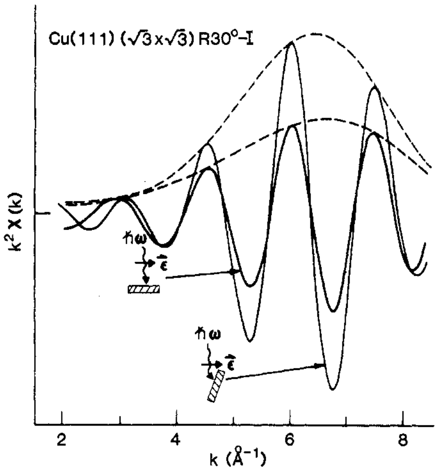

Fig. 6. Processed SEXAFS data for I adsorbed on Cu(111), showing how the amplitude of the SEXAFS oscillations above the I L_3 edge varies with orientation of the electric polarization vector $\boldsymbol{\epsilon}$ relative to the surface normal. Detailed analysis permits determination of the I site geometry in addition to the Cu–I spacing. This experiment involved a one-third coverage of the surface with an I overlayer whose unit cell was related to the underlying unit cell by $\sqrt{3} \times \sqrt{3}$ rotated 30°. [From Citrin *et al.* (*11*)]

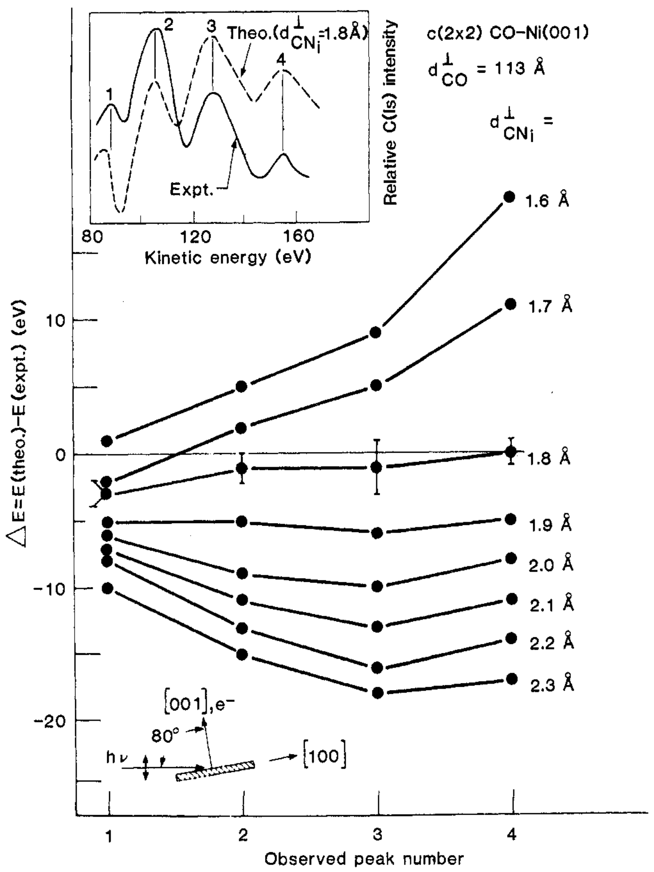

Fig. 5. Normal photoelectron diffraction for the carbon 1*s* level for CO on Ni(100). (Inset) Comparison of the measured spectrum (full curve) with a calculated spectrum (dashed curve) assuming a C–Ni spacing of 1.8 Å. The sensitivity to the C–Ni spacing is shown in the main part of the figure, where the deviation between the experimental and theoretical peak positions is plotted for various trial values of the spacing. [From Kevan *et al.* (*10*)]

Photoelectron Diffraction

The physical basis of the PhD technique is illustrated in Fig. 4a. When the photoelectron wave emitted directly from the core level in an adsorbate species interferes coherently with waves scattered from surrounding adsorbate and substrate atoms, the emitted intensity varies with emission angle and photoelectron energy (and thus wavelength) in a fashion that is determined by the local structural environment of the emitter relative to these surrounding atoms. Measurements of both the angular dependence at fixed photon energy (*8*) and the energy dependence at fixed emission angle (*9*) demonstrate significant variations due to this effect and can be compared with theoretical calculations based on various assumed local structures. This "internal diffraction" phenomenon has much in common with another surface technique, low-energy electron diffraction (LEED), although the fact that emission is from the atom whose location is of interest is a potential advantage in structural sensitivity. Moreover, a recent application of the technique, described below, indicates that PhD from individual atoms within a molecule may be more sensitive to the location of the atom relative to the substrate than to its position within the molecule, allowing each location to be determined independently.

Figure 5 illustrates some data from a study of carbon monoxide adsorption on a Ni(100) surface *(10)*. In the inset, the intensity of emission for the C 1*s* state normal to the surface is shown as a function of photoelectron kinetic energy. The PhD modulations are also shown by theoretical calculations, and the main part of Fig. 5 shows how the locations of the peaks in the spectrum (arbitrarily numbered) deviate from those in the calculations as the separation of the carbon atom and top nickel atom layer is varied. The results support the view that the CO molecules are bonded linearly on top of surface Ni atoms with the C end "down" and a C–Ni separation of 1.8 Å. While these calculations are rather insensitive to the oxygen atom locations, separate data on PhD from the oxygen 1*s* level are consistent with a C–O separation equal to that in the free CO molecule (1.13 Å). Experiments near the C and O 1*s* levels are extremely difficult to carry out at present, but study of these important species in adsorbed molecules should be eased by the new generation of radiation sources.

Surface EXAFS

While PhD involves the interference between emitted and scattered photoelectron waves as seen at a detector outside a surface, SEXAFS involves the same interference at the emitter site itself (Fig. 4b). Modulations in the wave field at the emitter with photoelectron energy and thus *k* lead to modulations in photoabsorption and secondary electron emission through the photoionization cross-section matrix elements. The photoabsorption cross section will be enhanced or diminished depending on whether the scattered waves arrive back at the origin in phase or out of phase with the outgoing wave. These modulations may be extracted as a fine-structure function χ, which has the form

$$\chi(k) = \sum_j A_j(k)\sin[2kR_j + \phi(k)] \quad (3)$$

where the sum over j is over atomic shells surrounding the emitter at distances R_j, and A_j and ϕ are amplitude and phase factors, which are species-dependent. After a minor correction for the k dependence of the phase factor, a Fourier transform of $\chi(k)$ can lead to a direct determination of the structural parameters R_j. This direct approach contrasts markedly with most surface structure techniques, which require comparison of experimental data and theoretical calculations based on a range of "guessed" model structures (as in PhD). There have been a number of demonstrations of this technique, but it is clear that the primary information is the nearest neighbor spacing, which does not, by itself, allow complete structural determination. Moreover, there are significant difficulties in obtaining the coordination number directly from the amplitude factors A_j. However, it was shown recently that the dependence of A_j on the direction of the polarization vectors of the incident photons can be used to determine local bonding sites. Figure 6 shows data from an experiment on the adsorption of iodine on Cu(111) *(11)*. The iodine L_3 edge fine-structure factor, scaled by k^2 and preprocessed by Fourier filtering to pick out the nearest neighbor scattering data, is shown for two different light polarizations. Evidently the periodicity is almost the same in each case, corresponding to the same I–Cu nearest neighbor spacing (found to be 2.66 Å, compared with 2.617 Å in bulk CuI), but the amplitude is different. The change of amplitude is consistent with adsorption of I in threefold hollow sites, and not in twofold bridge sites or onefold sites above the top layer of Cu atoms.

Strictly, the SEXAFS formula given above contains only single backscattering events and is appropriate for photoelectron energies above ~ 50 to 100 eV. The near-edge structure, however, also contains structural information, and because multiple scattering is important, information is available not only on two-body but also on three-body correlations. Some progress is being made in the interpretation of this x-ray absorption near-edge structure (XANES) *(12)* and may contribute to future generations of experiments. In addition, in the near-edge structure for adsorbed molecules, intramolecular scattering events or shape resonances may be observed. Once again, these effects can be sensitive to the direction of the light polarization vectors relative to a molecular axis, thus providing information on molecular orientation. Figure 7 shows such data

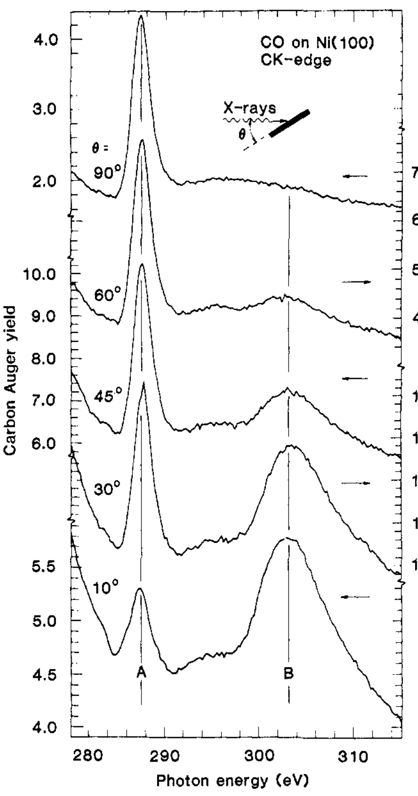

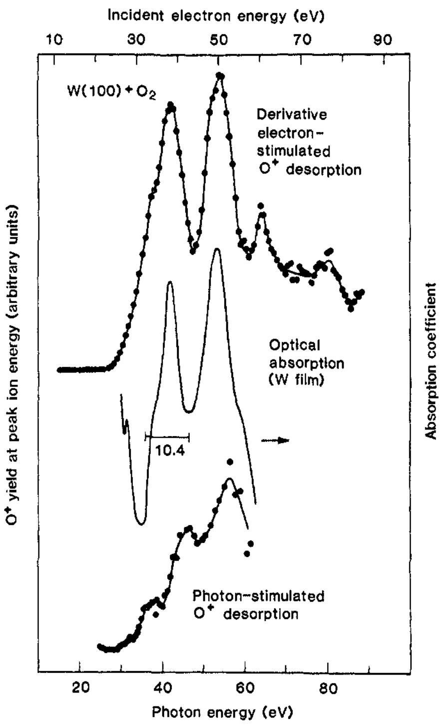

Fig. 7 (left). XANES data obtained for CO adsorbed on Ni(100) by monitoring the Auger yield in the vicinity of the carbon *K* edge. Peaks *A* and *B* are due to transitions from the carbon 1*s* level into "shape resonances" of π and σ symmetry, respectively, which arise through multiple scattering within the molecule. The dependence on photon polarization permits determination of the orientation of the CO molecule. [From Stöhr *et al.* *(13)*] Fig. 8 (right). Photon-stimulated desorption yield of O$^+$ ions from O adsorbed on the W(100) surface as a function of photon energy. Also shown are the optical absorption spectrum for bulk W and the derivative of the O$^+$ yield spectrum obtained by electron-stimulated desorption. The prominent peaks in the range 30 to 60 eV are associated with the W 4*f* and 5*p* core levels and demonstrate that desorption proceeds through an interatomic Auger mechanism.

(*13*) for the case of CO adsorption on Ni(100) discussed earlier, also in the vicinity of the C 1*s* core level. Two shape resonances are seen, the first involving excitation to a molecular bound state of π symmetry below the vacuum level, the second to a scattering resonance of σ symmetry overlapping the continuum. The data of Fig. 7 illustrate the sensitivity of these resonances to the direction of the polarization vector and confirm, by comparison with simple theory, the orientation of the CO molecule normal to the surface. The cross sections for transitions into the π and σ states are expected to vary, respectively, as $\sin^2\gamma$ and $\cos^2\gamma$, where γ is the angle between the electric polarization vector and the CO molecular axis. Similar shape resonances and their associated angular dependence have also been studied by excitation from shallower occupied molecular orbital states at photon energies in the softer ultraviolet range (*14*).

Photon-Stimulated Desorption

While the desorption of ions of adsorbate species, particularly positively charged ions, has long been known to be possible by incident electron stimulation (electron-stimulated desorption or ESD), the demonstration that the same process, involving the same initial electronic excitation, can be achieved with incident photons is relatively recent. Because of different cross-section behavior, thresholds are much sharper in PSD than in ESD. Thus the demonstration of the equivalence of PSD and ESD has yielded improved information on the threshold energies, and hence on the physics of the processes involved. In particular, it was proposed (*15*) recently that one process involved in positive ion desorption is the loss of two or more electrons from an adsorbate species in the Auger decay following a core state ionization. Moreover, in the case of highly ionic oxides, it was suggested that O^+ desorption could be produced by an interatomic Auger transition involving initial core state ionization of the metal cation. A clear demonstration of this process is seen in Fig. 8, which shows the PSD yield of O^+ from an oxygenated W(100) surface as a function of photon energy (*16*). The yield shows considerable structure correlated with the W 4*f* and 5*p* levels, which are also seen in the optical absorption spectrum for bulk W. Because the ESD cross sections rise over a wide energy range these core level thresholds are not readily visible in a raw ESD excitation spectrum, although, as shown, a differential of such an ESD spectrum does show these interatomic thresholds.

In addition to allowing the study of electronic thresholds and bonding character, studies of the PSD ion angular distributions (PSDIAD), like the ESD ones (*17*), provide clear information on local bonding geometry if it is assumed that emission of the desorbed ion will occur primarily along the direction of the broken bonds. Moveover, the process of PSD involving Auger decay of a core hole means that PSD yields can monitor SEXAFS of the relevant core-level photoionization cross section. A recent demonstration of the effect is the detection of PSD SEXAFS in the O^+ yield from a Mo(100) surface above the molybdenum L_1 edge (*18*); because it involves the interatomic Auger process, the method provides a means of sampling the structural environment of only those substrate atoms bonded to the desorbing adsorbate, a feature also demonstrated by the recent study.

Future Directions

The examples of recent achievements outlined above were selected because they illustrate strong current trends. Each type of experiment will profit from the high brightness of the new sources. In addition, there are some interesting future directions that are not so well illustrated in current work. For example, some surface scientists are eager to break away from the purely static techniques discussed above and to use synchrotron radiation methods to study the dynamics of surfaces. One possibility would be to perform very fast photoemission measurements and monitor the progress of surface chemical reactions in real time. We envisage here repetitive experiments involving pulsed molecular beams or pulsed laser sources to initiate chemical reactions.

The vibrational modes of surface chemical species represent another area of surface dynamics. The most popular technique in use in this case is high-resolution electron energy loss spectroscopy. Its ultimate resolution, however, is limited by electron energy analysis technology to a few millielectron volts. The alternative technique of infrared absorption spectroscopy does not suffer from this limitation. It seems likely that synchrotron radiation, used as an infrared source, can revitalize and extend this older technique.

Other important directions include studies of the magnetic properties of surfaces through spin-polarized photoemission and studies of surfaces with very fine spatial resolution. The latter could be of considerable technological value in the characterization of microelectronic systems and compositionally modulated structures such as those made by molecular-beam epitaxy. Finally, some of the photoemission spectroscopies that are directed toward the determination of surface atomic structures might be supplanted by developments in glancing-incidence surface x-ray diffraction (*19*). In this case photoemission would revert predominantly to its original purpose, namely the study of electronic rather than structural properties. The new synchrotron sources thus offer exciting prospects and challenges in the area of surface science.

References and Notes

1. For a survey of the properties of synchrotron radiation and its applications, see *Phys. Today* **34** (May 1981).
2. P. Eisenberger and B. M. Kincaid, *Science* **200**, 1441 (1978).
3. T. M. Duc, C. Guillot, Y. Lassailly, J. Lecante, Y. Jugnet, J. C. Vedrine, *Phys. Rev. Lett.* **43**, 789 (1979); P. H. Citrin, G. K. Wertheim, Y. Baer, *ibid.* **41**, 1425 (1978).
4. J. F. van der Veen, P. Heimann, F. J. Himpsel, D. E. Eastman, *Solid State Commun.* **37**, 555 (1981).
5. M. I. Holmes and T. Gustafsson, *Phys. Rev. Lett.* **47**, 443 (1981).
6. M. Posternak, H. Krakauer, A. J. Freeman, D. D. Koelling, *Phys. Rev. B* **21**, 5601 (1980).
7. T. E. Felter, R. A. Barker, P. J. Estrup, *Phys. Rev. Lett.* **38**, 1138 (1977); M. K. Debe and D. A. King, *J. Phys. C* **10**, L303 (1977); E. Tosatti, *Solid State Commun.* **25**, 637 (1978); J. E. Inglesfield, *J. Phys. C* **11**, L69 (1978).
8. N. V. Smith, H. H. Farrell, M. M. Traum, D. P. Woodruff, D. Norman, M. S. Woolfson, B. W. Holland, *Phys. Rev. B* **21**, 3119 (1980).
9. S. D. Kevan, D. M. Rosenblatt, D. Denley, B. C. Lu, D. A. Shirley, *Phys. Rev Lett.* **41**, 1565 (1978).
10. S. D. Kevan, R. F. Davis, D. M. Rosenblatt, T. G. Tobin, M. G. Mason, D. A. Shirley, C. H. Li, S. Y. Tong, *ibid.* **46**, 1629 (1981).
11. P. H. Citrin, P. Eisenberger, R. C. Hewitt, *ibid.* **45**, 1948 (1980).
12. P. J. Durham, J. B. Pendry, C. H. Hodges, *Solid State Commun.* **38**, 159 (1981).
13. J. Stöhr, K. Baberschke, R. Jaeger, R. Treichler, S. Brennan, *Phys. Rev. Lett.* **47**, 381 (1981).
14. E. W. Plummer and T. Gustafsson, *Science* **198**, 165 (1977).
15. M. L. Knotek and P. J. Feibelman, *Phys. Rev. Lett.* **40**, 964 (1978).
16. D. P. Woodruff, P. D. Johnson, M. M. Traum, H. H. Farrell, N. V. Smith, R. L. Benbow, Z. Hurych, *Surf. Sci.* **104**, 282 (1981).
17. T. E. Madey, R. Stockbauer, J. F. van der Veen, D. E. Eastman, *Phys. Rev. Lett.* **45**, 187 (1980).
18. R. Jaeger, J. Feldhaus, J. Haase, J. Stöhr, Z. Hussain, D. Menzel, D. Norman, *ibid.*, p. 1870.
19. P. Eisenberger and W. C. Marra, *ibid.* **46**, 1081 (1981).